thermodynamic parameters derived from NMR data to those obtained from more conventional experiments, to attempt to establish the relationship existing between thermodynamics and molecular interactions.

References and Notes

(1) M. Daoud, J. P. Cotton, B. Farnoux, G. Jannink, G. Sarma, H. Benoit, C. Duplessix, C. Picot, and P. G. De Gennes, *Macromolecules*, **8**, 804 (1975).
(2) H. Benoit, R. Duplessix, R. Ober, M. Daoud, J. P. Cotton, B. Farnoux, and G. Jannink, *Macromolecules*, **8**, 451 (1975).
(3) B. E. Eichinger and P. J. Flory, *Trans. Faraday Soc.*, **64**, 2035 (1968).
(4) P. J. Flory, "Statistical Mechanics of Chain Molecules", Interscience, New York, N.Y., 1969.
(5) M. L Huggins, *J. Chem. Phys.*, **9**, 440 (1941).
(6) P. J. Flory, *J. Chem. Phys.*, **9**, 660 (1941).
(7) M. L. Huggins, *Polym. J.*, **4**, 511 (1973).
(8) M. Daoud and G. Jannink, *J. Phys. (Paris)*, **37**, 973 (1976).
(9) J. P. Cohen-Addad and C. Roby, *J. Chem. Phys.*, **63**, 3095 (1975).
(10) J. P. Cohen-Addad and R. Vogin, *Phys. Rev. Lett.*, **33**, 940 (1974).
(11) J. P. Cohen-Addad and J. P. Faure, *J. Chem. Phys.*, **61**, 1571 (1974).
(12) J. P. Cohen-Addad, *J. Chem. Phys.*, **64**, 3438 (1976).
(13) W. W. Graessley, "The Entanglement Concept in Polymer Rheology", Vol. 16, Springer Verlag, New York, N.Y., 1974.
(14) E. A. Guggenheim, *Trans. Faraday Soc.*, **44**, 1007 (1948).
(15) Y.-K. Leung and B. E. Eichinger, *Macromolecules*, **7**, 685 (1974).
(16) T. G. Fox and P. J. Flory, *J. Am. Chem. Soc.*, **73**, 1909 (1951).
(17) C. E. H. Bawn and R. D. Patel, *Trans. Faraday Soc.*, **52**, 1664 (1956).
(18) C. E. H. Bawn, E. S. Hill, and M. A. Wajid, *Trans. Faraday Soc.*, **52**, 1651 (1956).
(19) B. E. Eichinger and P. J. Flory, *Trans. Faraday Soc.*, **64**, 2053 (1968).
(20) B. E. Eichinger and P. J. Flory, *Trans. Faraday Soc.*, **64**, 2061 (1968).

Proton and Carbon-13 Spin–Lattice Relaxation Studies of the Conformation and Dynamical Behavior of Poly(4-vinylpyridine) in Methanol Solution

Denis Ghesquière,[1a] Buu Ban,[1b] and Claude Chachaty*[1a]

Service de Chimie Physique, C.E.N. de Saclay, 91190 Gif-sur-Yvette, France.

Received January 31, 1977

ABSTRACT: The segmental motions of poly(4-vinylpyridine) in CD_3OD solution have been investigated between 220 and 350 K by ^{13}C and ^{1}H spin–lattice relaxation. The experiments were performed at 25 MHz (^{13}C) and 100 and 250 MHz (^{1}H). While the relaxations of ^{1}H and ^{13}C of the main chain are interpretable in terms of an isotropic segmental motion assuming a temperature-dependent distribution of correlation times, this simple model does not hold for the pyridyl group. Theoretical expressions for ^{1}H and ^{13}C relaxation rates have been derived to interpret the anisotropic motion of this group undergoing oscillations of limited amplitude about the N–C_4 axis. The length and orientation of all internuclear vectors have been computed for the different triads included in rrmrr and rrrmr sequences. In these calculations the oscillation amplitude α of the pyridyl ring, its temperature dependence, the relevant activation energy E_G, as well as the activation energy E_R of the isotropic motion of a segment of the macromolecular chain were taken as adjustable parameters. The best consistency between the relaxation data at different frequencies was given by $E_G \simeq 3$ kcal mol^{-1}, $E_R \simeq 4$ kcal mol^{-1}, and $50° < \alpha < 80°$.

(I) Introduction

Most of the recent NMR works on the molecular dynamics of polymers in solution have been performed by T_1 and T_2 relaxation times and nuclear Overhauser effect measurements on ^{13}C.[2-12] The T_2 relaxation time cannot be determined with sufficient accuracy whenever the NMR line width is due to an unresolved fine structure as in the case of most of the atactic polymers. The nuclear Overhauser effect of ^{13}C appears as a subsidiary method of studying the molecular motion in the domain of correlation times of 10^{-10} to 10^{-8}s, characteristic of many polymers in solution, but is the less accurate of the relaxation methods and its use is not essential if T_1 measurements may be done at different spectrometer frequencies. Although difficult to interpret, the proton spin–lattice relaxation provides information on the molecular motions and local conformations of polymers since it strongly depends on interproton distances.

In the present work, the ^{13}C and ^{1}H spin–lattice relaxations of atactic poly(4-vinylpyridine) (P4VP) in methanol solution have been studied as a function of temperature at 25 MHz and 100 and 250 MHz, respectively, in order to compare the segmental motion with that of the same polymer quaternized by H^+ and alkyl bromides which will be reported hereafter. The relaxation data have been interpreted with the help of a theoretical model of restricted motion derived from a previous study on molecular motions in the solid state.[13] Although a previous work on poly(2-vinylpyridine) (P2VP) has shown that ^{13}C relaxation is virtually independent on the polymer tacticity,[11] this is not expected to be true for ^{1}H relaxation so that we have carried out some conformational energy calculations to determine the interproton distances in the most typical sequences of an atactic polymer.

(II) Experimental Procedure

The 4-vinylpyridine from Fluka was distilled twice under reduced pressure in the presence of calcium hydride. The polymerization initiated by azobis(isobutyronitrile) was performed under vacuum in methanol solution at 60 °C. The polymer was recovered and purified by successive precipitation by ethyl ether from methanol solutions. The molecular weights were determined by viscosimetry of ethanol solutions at 25 °C using the relation of Berkowitz et al.[14] The molecular weights of the polymers under study were 75 000, 132 000, 150 000, and 222 000. The NMR experiments were performed in Fourier transform with a Cameca TSN 250 spectrometer (ν_H 250 MHz) and a Varian XL100-12 WG spectrometer ($\nu_{^{13}C}$ 25.15 MHz, ν_H 100 MHz). The T_1 relaxation times were measured by inversion recovery (180°–τ–90° sequence) or in the case of ^{13}C by the Freeman and Hill[15] sequence ($90°_{\infty}, t \gg T_1, 180°, \tau, 90°, \ldots$). The recovery time between two sequences was taken at least five times longer than the estimated value of T_1 given by preliminary experiments. All measurements were done in CD_3OD solutions, the magnetic field being locked on the deuterium resonance. The ^{13}C NMR spectra were recorded under complete noise decoupling of protons. All T_1 mea-

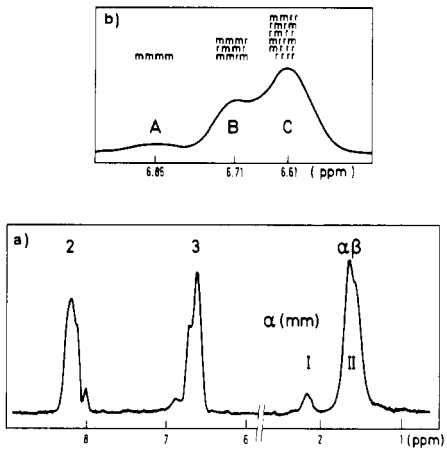

Figure 1. (a) ^1H 250 MHz NMR sepctrum of atactic P4VP in CD_3OD. The chemical shifts are given in ppm from TMS. (b) Expansion of the H_3 resonance with pentad assignments.

Table I
Pentad Tacticity of P4VP Deduced from ^1H and ^{13}C NMR Spectra

Calcd[a]	H_α (Figure 1)	H_3 (Figure 1) $^{13}C_4$ (Figure 2)	
mmmm 0.05	3I/(I + II) = 0.22	0.06 (peak A)	0.37 (peak a)
mmmr 0.11			
rmmr 0.06		0.31 (peak B)	
mmrm 0.12			
mmrr 0.12		0.63 (peak C)	0.34 (peak b)
rmrm 0.12			
rmrr 0.14			
mrrm 0.06			0.29 (peak c)
mrrr 0.14			
rrrr 0.08			

[a] From Bernouillan statistics with $P_m = 0.47$ (see text).

surements have been performed at least three times on different samples. The temperature of the probe was calibrated either with a methanol standard sample or with a copper–constantan thermocouple.

(III) Results

(1) Tacticity of the Polymer. While isotactic and atactic P2VP have been subjected to several NMR studies,[16–18] to our knowledge P4VP has been obtained only in the atactic form and its ^1H and ^{13}C NMR spectra have not been fully analyzed. The interpretation of ^1H and ^{13}C NMR spectra in terms of the tacticity of this polymer may be given nevertheless in analogy with P2VP. It is possible in particular to assign the weak single line at 2.17 ppm of the proton NMR spectrum of P4VP to the methine proton H_α of isotactic triads (Figure 1). The area S_I of this line compared to the one of the unresolved band of the H_α and H_β protons S_{II} gives a straightforward determination of the proportion of isotactic triads:

$$\%\,\mathrm{mm} = 3 \times \frac{S_I}{S_I + S_{II}} \times 100 \qquad (1)$$

we have found (mm) = 22%, the probabilities of isotactic and

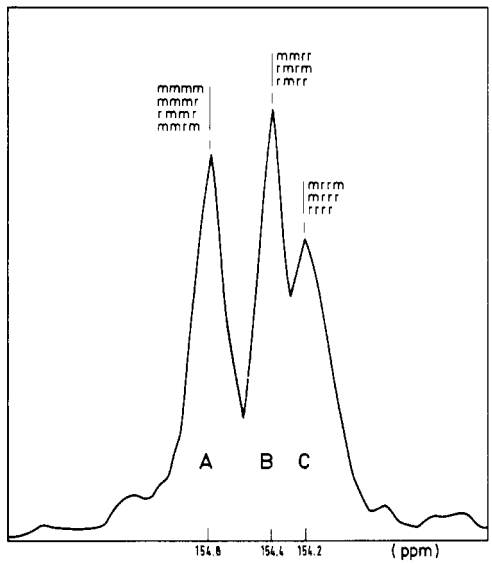

Figure 2. ^{13}C NMR spectrum of the C_4 quaternary carbon of the pyridyl ring in CD_3OD at 26 °C. The chemical shifts are in ppm from TMS.

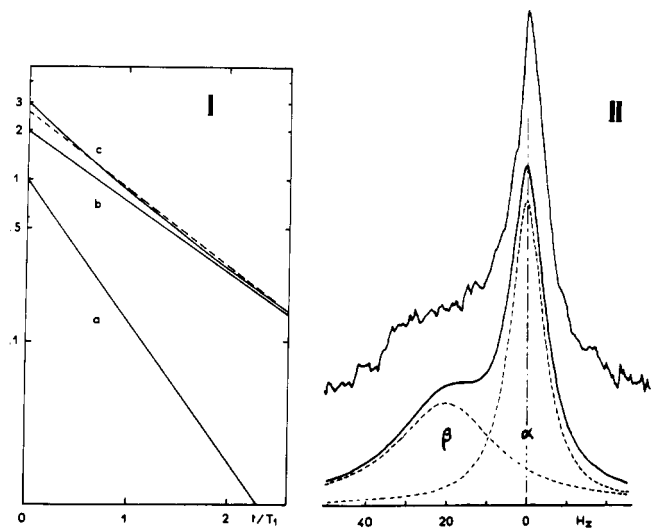

Figure 3. (I) theoretical semilog plot of the recovery of the magnetization of C_α and C_β after a 180° pulse (arbitrary units). The C_β (a) and C_α (b) resonances are assumed to be superimposed giving a single line $C_{\alpha\beta}$ (c). The dotted straight line gives the mean slope of the curve (c). (II) simulated spectrum of $C_{\alpha\beta}$ assuming $\delta_\alpha - \delta_\beta = 20$ Hz, $(\Delta\nu_{1/2})_\alpha = 10$ Hz and $(\Delta\nu_{1/2})_\beta = 30$ Hz

syndiotactic addition being therefore $P_m = 0.47$ and $P_r = 0.53$, respectively. The resonances of H_2 and H_3 show a structure due to the tacticity of the polymer. The relative intensities of the three peaks of H_3 do not correspond to a triad structure since they are inconsistent with the tacticity given above, so that they have been tentatively assigned to a partially resolved pentane structure (Table I).

Several interpretations of the ^{13}C NMR of atactic P2VP have been proposed.[16–18] The ^{13}C spectrum of this polymer obtained in our laboratory is in agreement with the ones published by Brigodiot et al.[16] and by Matsuzaki et al.[17] and does not show the weak line located at the low field side of the main three lines of the quaternary carbon as in the spectrum published by Lukovkin et al.[18] In the ^{13}C NMR spectrum of P4VP the structure of the resonance of the quaternary carbon is very similar to the one of the atactic P2VP (Figure 2). The assignment of the three lines of the quaternary carbon to mm, mr, and rr triads is inconsistent with the proton NMR spec-

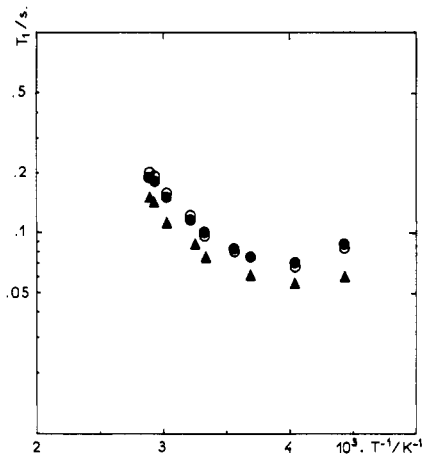

Figure 4. Semilog plot of T_1 vs. T^{-1} for P4VP in CD_3OD solution: carbon 2 (○), carbon 3 (●), and aliphatic carbons $C_{\alpha\beta}$ (▲). Concentration 1 M in monomer units, M_w = 75 000.

trum of our polymer and they correspond likely to the overlap of peaks corresponding to pentads as determined by the relevant calculated probabilities given in Table I. A similar interpretation is given by Matsuzaki et al.[17] in the case of P2VP.

(2) ^{13}C Relaxation. The semilogarithmic plot of the recovery of the ^{13}C nuclear magnetization after a 180° pulse is nearly linear for all carbons including the methine (C_α) and methylene (C_β) carbons of the aliphatic chain although their resonances are superimposed. Assuming that the relaxation time T_1 of C_α is twice the one of C_β as observed in the case of isotactic P2VP[11] where the corresponding resonances are separated, it appears that the recovery of the $C_{\alpha\beta}$ resonance is governed by the relaxation time of C_α which may be therefore underestimated. To estimate the error in the determination of $T_{1\alpha}$, we have simulated the dependence of the $C_{\alpha\beta}$ resonance as a function of the time delay τ between a 180° and a 90° pulse in a relaxation experiment. The semilogarithmic plots shown in Figure 3I have been calculated for the most unfavorable case where C_α and C_β are exactly superimposed, taking $T_{1\beta} = \frac{1}{2}T_{1\alpha}$ and $(I_0)_\beta = (I_0)_\alpha/2$, where I are the signal amplitudes (assuming that $(\Delta\nu_{1/2})_\beta = 2(\Delta\nu_{1/2})_\alpha$).

It may be seen that the curve calculated for $C_{\alpha\beta}$ fits approximately a straight line (dotted line), the apparent T_1 being nearly equal to $0.9T_{1\alpha}$. In reality the C_α and C_β resonances are not exactly superimposed and their overlapping resonances are satisfactorily simulated with $\delta_\alpha - \delta_\beta$ = 20 Hz, $(\Delta\nu_{1/2})_\alpha$ = 10 Hz, and $(\Delta\nu_{1/2})_\beta$ = 30 Hz (Figure 3II) so that a similar treatment yields $(T_1)_{\alpha\beta} \simeq 0.96T_{1\alpha}$. Considering that the experimental uncertainty in the determination of T_1 of the order of 0.1 s is about 10%, we can assume that the apparent T_1 of the $C_{\alpha\beta}$ resonance is virtually the one for C_α. The dependence of the relaxation times on the reciprocal of the temperature between 220 and 350 K given in Figure 4 will be discussed in section IV. We did not observe any concentration dependence of the relaxation times for 0.5 to 4.0 M solution of the polymer (concentration in monomer units) at 27 °C.

(3) Proton Relaxation. The temperature dependence of the proton relaxation time has been determined at 100 and 250 MHz (Figure 5). A typical recording of an inversion recovery experiment at 250 MHz is given in Figure 6 together with the semilogarithmic plot of the magnetization which is nearly linear even for the superimposed α and β proton resonances. The simple way of estimating the individual relaxation times of H_α and H_β reported for $^{13}C_\alpha$ does not hold since the line shapes of the corresponding resonances are unknown. It seems however most likely that the recovery of the $H_{\alpha\beta}$ resonance after a 180° pulse is governed by H_α, the relaxation time of which may be two or three times longer than the one of H_β. This is well confirmed by the fact that the apparent relaxation time of the $H_{\alpha\beta}$ is close to the one of the H_α of the isotactic triads which is observed separately. The comparatively high sensitivity of the ^1H NMR allowed us to extend to low polymer concentrations the T_1 relaxation time measurements. It has been found that the relaxation of all protons is virtually independent of the concentration in a range of 0.03 to 2.0 M at 24 °C.

(IV) Discussion

(1) Conformational Energy Calculations. It is necessary for the interpretation of relaxation data to know the preferential conformations of the polymer and to estimate the energy required for segmental motions. This has been done by use of the SIMPLEX program[19–21] which provides the most stable conformation of the molecules corresponding to energy minima. The total energy considered is the sum of the torsional energy $V = \frac{1}{2}V_0(1 - \cos n\theta)$, the van der Waals energy $E_{VDW} = A\exp(-Br) - Cr^{-6}$, and the electrostatic energy $E_e = 322qq'/Dr$, D being the dielectric constant of the medium, r an internuclear distance, and θ a torsion angle. The energy maps about equilibrium conformations are provided by the DESCARTES program.[22] While SIMPLEX has been applied to hexads, the use of DESCARTES was restricted to tetrads since calculations on hexads would be too time consuming.

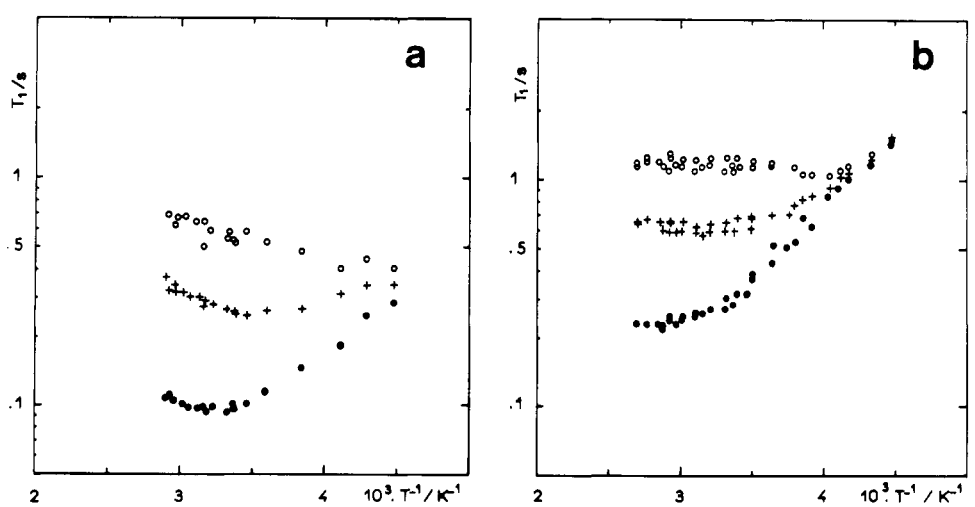

Figure 5. Semilog plot of T_1 vs. T^{-1} at 100 MHz (a) and 250 MHz (b) for H_2 (○), H_3 (+), and $H_{\alpha\beta}$ (●). Concentration 1 M in monomer units and M_w = 75 000.

Table II

(a) Definition of Angles for the rrrmr Sequence

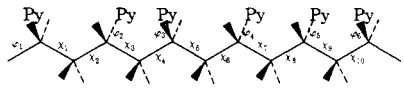

(b) Stable Conformations from SIMPLEX Program

	χ_1	χ_2	χ_3	χ_4	χ_5	χ_6	χ_7	χ_8	χ_9	χ_{10}	φ_1	φ_2	φ_3	φ_4	φ_5	φ_6
rrrmr (D = 3.5)	0	1	−3	3	3	7	35	3	−2	2	0	−3	2	3	−1	1
rrrmr (D = 20)	0	2	−1	0	2	3	105	2	−2	−2	0	−1	−1	1	−1	1
rrmrr (D = 20)	0	2	3	−2	104	−1	3	3	−2	0	0	1	2	−1	0	0

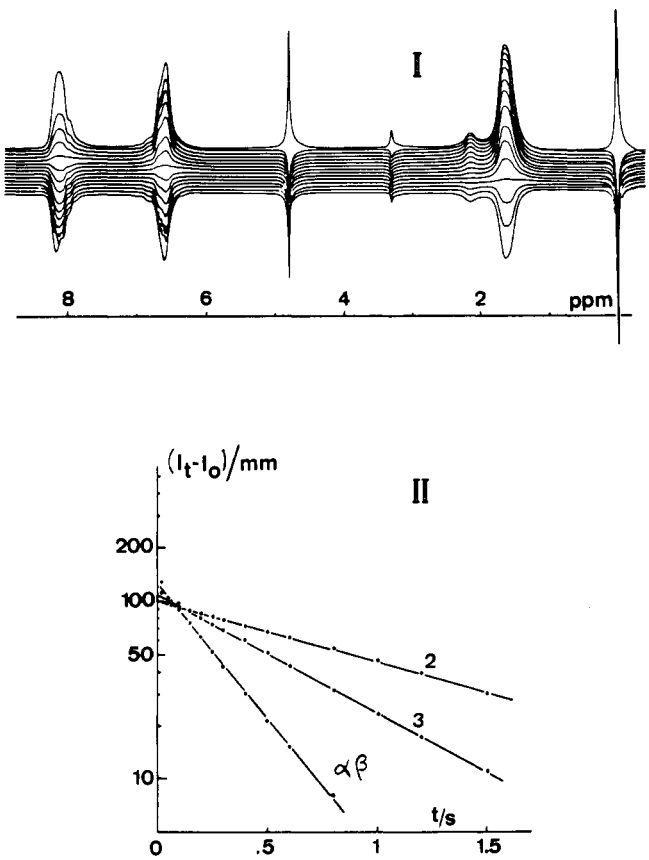

Figure 6. (I) Stereoscopic display of an inversion recovery experiment on ^1H at 250 MHz. The time delay between 180 and 90° pulses are: 8, 1.5, 1.2, 1.0, 0.8, 0.6, 0.5, 0.4, 0.3, 0.25, 0.2, 0.15, 0.10, 0.06, and 0.02 s. The time delay between the sequences is 8 s. (II) Corresponding semilog plot of the magnetization recovery.

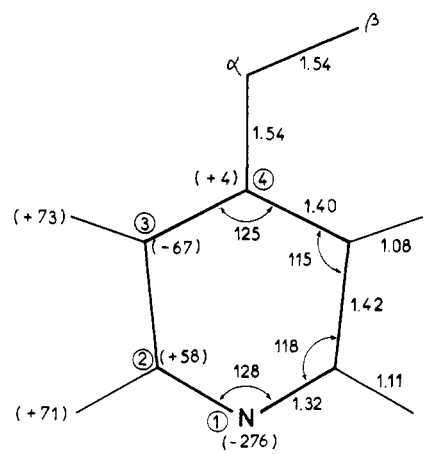

Figure 7. Geometry and charge density distribution of the pyridyl ring taken from ref 23 and 24, respectively. The distances are given in ångström units and the angles in degrees. The charge densities in parentheses are multiplied by 10^3.

In these calculations the geometry of the aliphatic main chain was given by: ∠CCC = ∠CCH = 109°47, r_{C-C} = 1.54 Å, and r_{C-H} = 1.09 Å. The geometry of the pyridyl ring was taken from ref 23. For this ring the electric charge distribution and the length of CH bonds were taken from ref 24. The charge densities given for the C_4–H fragment of pyridine were concentrated on C_4 and the C_4–C_α distance was taken equal to 1.54 Å (Figure 7). For the determination of the most stable conformations we have considered the rrrmr and rrmrr sequences which seem the most representative of our atactic polymer. These two hexads give similar results about the local conformation of the polymer which is shown in Table II according to the following convention: the torsion angle χ_i = 0 corresponds to a trans conformation of the carbon backbone of the main chain and the torsion angle φ_i = 0 corresponds to the methine proton H_α of this chain in the plane of the adjacent pyridyl ring.

The calculations of equilibrium conformations have first been made with the most widely assumed value D = 3.5 giving χ_7 = +35° (Table II) and our results are in good agreement with those of Panov et al.[25] However, Kirsh et al.[26] and more recently Štrop et al.[27] have shown that for P4VP in alcohol solutions D = 20–30 is more probable. Taking D = 20 we have found a preferential gt conformation for the meso diad with χ_7 = 105° (Table II). Our experimental results are actually more consistent with the conformations calculated with D = 20 than the ones derived on taking D = 3.5.

The conformational energy maps obtained by the DESCARTES program on rrr and rmr tetrads indicate the same stable conformations as the SIMPLEX program. Figure 8 shows that the rr sequence corresponds to a tt conformation (map I) whereas the rm sequence gives besides the most stable gt conformation (χ_7 = 105°, χ_8 = 0°) three other conformations with an energy 1 kcal mol^{-1} higher: χ_7 = 45° and χ_8 = 0, χ_7 = 15° and χ_8 = −30°, χ_7 = 15° and χ_8 = −85° (map III). As expected from a previous work on P2VP[11] the maps II and IV indicate that the α proton is in the plane of the pyridyl ring.

An inspection of conformational energy maps suggests moreover that a 360° rotation about any single bond is most unlikely since it needs an energy higher than 10 kcal mol^{-1} whereas segmental motions of the polymer with activation energies smaller than 5 kcal mol^{-1} are restricted to oscillations about equilibrium positions.

(2) Segmental Motion of the Main Chain. The relaxation times T_1 of the protons and carbons of the main chain have been interpreted in terms of isotropic motion of polymer segments consisting of a small number of monomer units. The overall reorientation correlation time of the macromolecule

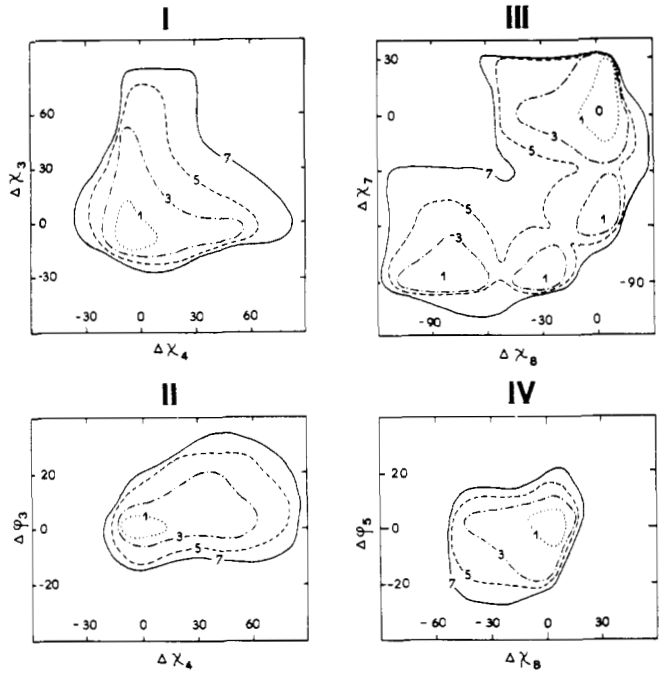

Figure 8. Conformational energy maps obtained by the Descartes program: (I and II) rr triad; (III and IV) mr triad. The horizontal and vertical scales indicate the deviations from equilibrium positions.

is probably of the order of 10^{-7}s or larger and does not contribute efficiently to the relaxation process. This is confirmed by the independence of T_1 upon molecular weights over 10 000 observed for other polymers[2a,7,9,28–30] and also in the present case (75 000 ≤ $\overline{M}_w$ ≤ 222 000). The isotropic character of the segmental motion of the aliphatic chain has been suggested for several vinyl polymers like for instance polystyrene,[2a,7] polyvinyl(2-vinylpyridine),[11] and polypropylene.[6] For an isotropic motion, the proton and ^{13}C spin–lattice relaxation times are given respectively by equations:

$$\left(\frac{1}{T_1}\right)_{H_i} = \frac{3}{10}\gamma_H^4\hbar^2\sum_j r_{ij}^{-6}\left[\frac{\tau_R}{1+\omega_H^2\tau_R^2}+\frac{4\tau_R}{1+4\omega_H^2\tau_R^2}\right] \quad (2)$$

$$\left(\frac{1}{T_1}\right)_C = \frac{N}{10}\hbar^2\gamma_H^2\gamma_C^2 r_{CH}^{-6}\left[\frac{\tau_R}{1+(\omega_H-\omega_C)^2\tau_R^2}+\frac{3\tau_R}{1+\omega_C^2\tau_R^2}+\frac{6\tau_R}{1+(\omega_H+\omega_C)^2\tau_R^2}\right] \quad (3)$$

where γ_H, ω_H and γ_C, ω_C are the gyromagnetic ratios and Larmor frequencies for proton and ^{13}C, respectively, τ_R is the isotropic reorientation correlation time of a polymer segment, r_{ij} is the distance of a proton i to any proton j, and r_{CH} is the distance of a carbon to $N = 1$ or $N = 2$ attached protons. For protons the minimum $(T_1)_{min} = 2.339\omega_H \times (\gamma_H^4\hbar^2\,\Sigma_j\, r_{ij}^{-6})^{-1}$ occurs at $(\tau_R)_{min} = 0.6157\omega_H^{-1}$.

For $\omega_C = 1.58 \times 10^8$ rad s^{-1} and $\omega_H = 6.28 \times 10^8$ rad s^{-1}, we have likewise, in the case of ^{13}C, $(\tau_R)_{min} = 5.0 \times 10^{-9}$ s and $(T_1)_{min} = 2.348 \times 10^{46} r_{CH}^6$ s, r_{CH} being given in centimeters.

When working at several spectrometer frequencies as in the present work, one must make a straightforward measurement of the activation energy of motion by determining the temperatures where T_1 passes through a minimum. The Arrhenius plot of τ_R obtained by this method yields $E_R = 3.95 \pm 0.5$ kcal mol^{-1} with a preexponential factor $(\tau_R)_0 = (1.9 \pm 1.25) \times 10^{-12}$ s (Figure 9).

The T^{-1} dependence of the proton spin–lattice relaxation time at 100 and 250 MHz has been satisfactorily calculated from the values of $(T_1)_{min}$ observed at both frequencies taking $E_R = 3.5$–3.6 kcal mol^{-1} and $(\tau_R)_0 = 2.3$–3.0×10^{-12} s. In the

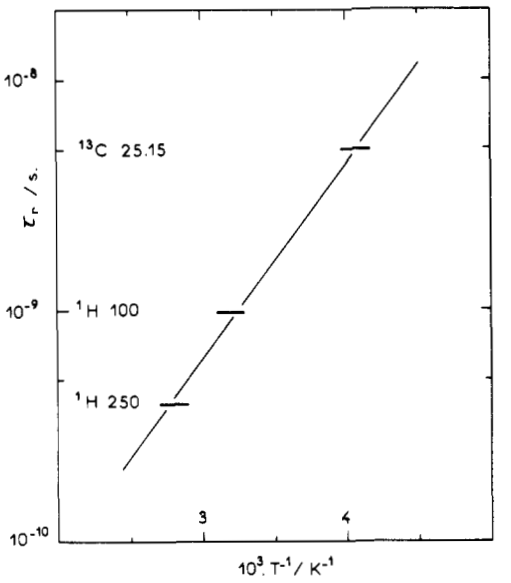

Figure 9. Arrhenius plot of τ_R deduced from T_1 minima at several spectrometer frequencies (MHz).

case of ^{13}C, the shape of the $T_1 = f(T^{-1})$ curve with the same parameters is also in agreement with the experimental one; however, the actual values of T_1 are larger by 20–30% than the calculated ones even taking $r_{CH} = 1.12$ Å for the aliphatic chain as suggested by the data of Bonham on n-heptane.[31]

We have attempted to account for this discrepancy by assuming a distribution of correlation times. The Fuoss–Kirkwood distribution of τ_R (see for instance ref 32 and 33) has been chosen as particularly convenient for our calculations, the proton and ^{13}C relaxation times being given respectively by

$$(T_1^{-1})_{H_i} = \frac{3}{10}\gamma_H^4\hbar^2\sum_j r_{ij}^{-6}\frac{\beta}{\omega_H}\left[\frac{(\omega_H\tau_R)^\beta}{1+(\omega_H\tau_R)^{2\beta}}+\frac{2(2\omega_H\tau_R)^\beta}{1+(2\omega_H\tau_R)^{2\beta}}\right] \quad (4)$$

$$(T_1^{-1})_C = \frac{N}{10}\hbar^2\gamma_H^2\gamma_C^2 r_{CH}^{-6}\beta\tau_R^\beta\left[\frac{(\omega_H-\tau_R)^{\beta-1}}{1+(\omega_H-\omega_C)^{2\beta}\tau_R^{2\beta}}+\frac{3\omega_C^{\beta-1}}{1+(\omega_C\tau_R)^{2\beta}}+\frac{6(\omega_C+\omega_H)^{\beta-1}}{1+(\omega_C+\omega_H)^{2\beta}\tau_R^{2\beta}}\right] \quad (5)$$

The best agreement between the experimental plots of T_1 vs. T^{-1} at the three spectrometer frequencies and the ones calculated from eq 4 and 5 were obtained by assuming a linear dependence upon T^{-1} of the distribution parameter β. Taking $E_R = 4.0$ kcal mol^{-1} and $(\tau_R)_0 = 1.3 \times 10^{-12}$ s, β was found to decrease from 0.95 to 0.65 between 3.0 and 4.5 10^{-3} K^{-1} (Figure 10). A narrowing of the correlation time distribution at increasing temperatures has also been proposed by Heatley and Begum[9] to account for the ^{13}C relaxation in the case of polystyrene and other vinyl polymers.

It may be pointed out in Figure 10 that the values of β corresponding to the $(T_1)_{min}$ observed for the protons at 100 and 250 MHz are close to unity so that the minimum values of T_1 are hardly affected by the distribution of correlation times in contrast with ^{13}C. For the protons of the main chain we have $(T_1)_{min} = 0.095$ and 0.230 s at 100 and 250 MHz, respectively. The conformational energy calculations yield for the α proton $0.22 < (T_1)_{min} < 0.25$ s at 250 MHz and $0.09 < (T_1)_{min} < 0.11$ s at 100 MHz, the upper limit corresponding to a mm sequence, confirming that the apparent relaxation time given by the $H_{\alpha\beta}$ resonance is in fact very close to the one of H_α as pointed out above.

(3) Anisotropic Motion of the Pyridyl Ring. It is seen on Figure 4 that the relaxation times of C_2 and C_3 are equivalent

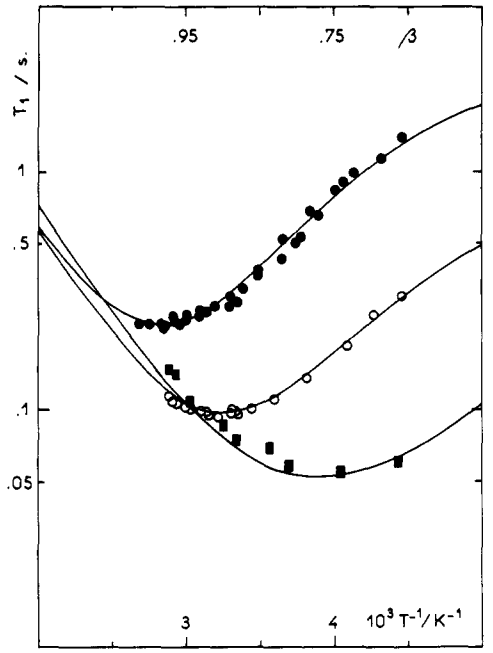

Figure 10. Simulation of the dependence of T_1 upon T^{-1} for the main chain carbons and protons with a correlation time distribution taking E_R = 4.0 kcal mol^{-1}, $(\tau_R)_0 = 1.3 \times 10^{-12}$ s, and the Fuoss–Kirkwood parameter varying linearly with T^{-1}. Experimental points: ^{1}H 250 MHz (●), ^{1}H 100 MHz (○), ^{13}C 25.15 MHz (■).

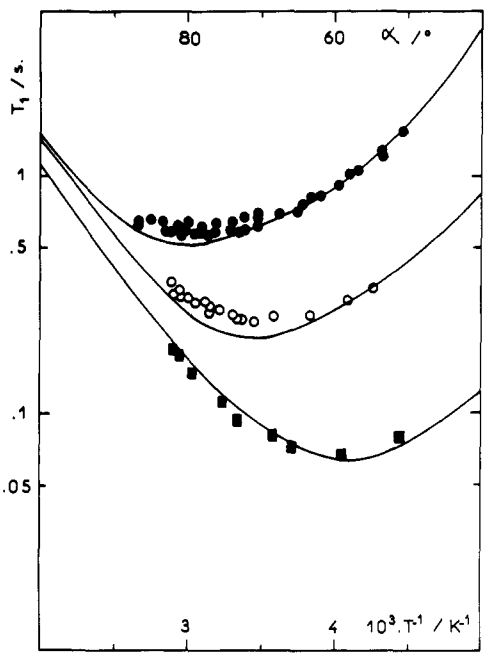

Figure 11. Simulation of the T^{-1} dependence of the T_1 of pyridyl H_3 at 250 MHz (●) and 100 MHz (○), of C_3 at 25.15 MHz (■), taking E_R = 4 kcal mol^{-1}, E_G = 3 kcal mol^{-1}, $(\tau_G)_0 = 9.7 \times 10^{-13}$ s, the angle α varying linearly with T^{-1}. The theoretical curves have been calculated with $(\tau_R)_0 = 1.3 \times 10^{-12}$ s for ^{1}H and 2.3×10^{-12} s for ^{13}C (see text).

within the limits of experimental errors. The situation is quite different for protons H_2 and H_3 (Figure 5). Assuming in a first step that the pyridyl groups have no motional freedom with respect to the main chain segments and undergo the same quasi-isotropic motion, we observe that in the whole range of temperatures the T_1 of H_2 is significantly smaller than the value expected from computed values of Σr_{ij}^{-6} involving the protons of the same monomer unit and of its two nearest neighbors. This is not a motional effect as it will be shown below but most likely a contribution of the dipolar interactions with protons of remote monomer units which come close to H_2 because of the folding motions of the chain. In the case of H_3 where the dipolar interactions occur mainly from the other protons of the same monomer unit and the ones of the two vicinal units, we observe a reverse behavior which is certainly not only an effect of correlation time distribution since it is unconsistent with the other nuclei of the ring.

It is known that one of the consequences of the anisotropic motion of a group is the rise of $(T_1)_{min}$ above the corresponding values expected for an isotropic motion (see for instance ref 2b). On the other hand the conformational energy maps of Figure 8 show that activation energies larger than 5 kcal mol^{-1} are needed to overcome the potential barriers surrounding the energy minima so that the motion of pyridyl rings about the C_4N axis must be considered as oscillations of comparatively small amplitude. We have therefore derived theoretical expressions of the dipolar relaxation rates of ^{1}H and ^{13}C for a rotational oscillation of HH or CH vectors about an axis Δ (see Appendix):

$$(T_1^{-1})_{H_i} = \frac{9}{80}\gamma_H^4\hbar^2 \sum_j r_{ij}^{-6} \left\{ [\tfrac{2}{3}(1 - 3\cos^2\gamma_{ij})^2 + \sin^2 2\gamma_{ij}(1 + \cos\alpha) + \sin^4\gamma_{ij}(1 + \cos 2\alpha)] \times \left(\frac{\tau_R}{1 + \omega_H^2\tau_R^2} + \frac{4\tau_R}{1 + 4\omega_H^2\tau_R^2} \right) + [\sin^2 2\gamma_{ij}(1 - \cos\alpha) + \sin^4\gamma_{ij}(1 - \cos 2\alpha)] \times \left(\frac{\tau_t}{1 + \omega_H^2\tau_t^2} + \frac{4\tau_t}{1 + 4\omega_H^2\tau_t^2} \right) \right\} \quad (6)$$

$$(T_1^{-1})_C = \frac{3}{80}N\gamma_H^2\gamma_C^2\hbar^2 r_{CH}^{-6} \left\{ [\tfrac{2}{3}(1 - 3\cos^2\gamma)^2 + \sin^2 2\gamma(1 + \cos\alpha) + \sin^4\gamma(1 + \cos 2\alpha)] \times \left(\frac{\tau_R}{1 + (\omega_H - \omega_C)^2\tau_R^2} + \frac{3\tau_R}{1 + \omega_C^2\tau_R^2} + \frac{6\tau_R}{1 + (\omega_C + \omega_H)^2\tau_R^2} \right) + [\sin^2 2\gamma(1 - \cos\alpha) + \sin^4\gamma(1 - \cos 2\alpha)] \times \left(\frac{\tau_t}{1 + (\omega_C - \omega_H)^2\tau_t^2} + \frac{3\tau_t}{1 + \omega_C^2\tau_t^2} + \frac{6\tau_t}{1 + (\omega_H + \omega_C)^2\tau_t^2} \right) \right\} \quad (7)$$

where γ is the angle between an internuclear vector and Δ, and α is the angular amplitude of the oscillation, and τ_t is the correlation time defined by $\tau_t^{-1} = \tau_R^{-1} + \tau_G^{-1}$, τ_G being the correlation time of the oscillation.

The parameters needed for the fitting of theoretical $T_1 = f(1/T)$ curves to experimental data are therefore α, $(\tau_G)_0$, and E_G, the preexponential factor and the activation energy of the oscillation. The parameters $(\tau_R)_0$ and E_R for the isotropic motion of the chain segment are given independently by the relaxation of H_α, H_β and C_α, C_β as shown in IV2.

The fitting of the $T_1 = f(1/T)$ curve of C_2 and C_3 to experimental points was obtained by seeking for a value of τ_G and the smallest possible value of α corresponding to $(T_1)_{min}$ observed and then by adjusting E_G and $(\tau_G)_0$ to obtain the best agreement in the whole temperature range. This procedure was carried out with an APL program allowing us to perform rapidly a large number of trials to determine the influence of all parameters. Several sets of parameters seem convenient to fit the ^{13}C relaxation data; however, the number of possible solutions is drastically reduced by the conditions of consistency with the relaxation of H_3 at 100 and 250 MHz.

A similar treatment was applied to the relaxation of H_3. All interproton distances less than 10 Å from the protons H_3 of

the central monomer unit of rr and rm triads where computed by the SIMPLEX program for the minimum energy conformation of the rrrmr and rrmrr sequences. To simplify the calculations of the proton relaxation times the interproton distances and γ_{ij} angles were taken invariant during the rotational oscillation about Δ. The best results were obtained for the rm triad which appears as the most representative of our polymers.

The T^{-1} dependencies of the T_1 relaxation times of H_3 at 250 and 100 MHz have been simulated by taking $E_G = 3.0$ kcal mol^{-1}, $(\tau_G)_0 = 9.7 \times 10^{-13}$ s, and an oscillation amplitude α varying linearly with T^{-1} from 50 to 80° between 220 and 350 K (Figure 11). This set of parameters holds satisfactorily for the C_2 and C_3 relaxation times taking however $(\tau_R)_0$, 2.3×10^{-12} s instead of $(\tau_R)_0 = 1.3 \times 10^{-12}$ s for H_3. Both values of $(\tau_R)_0$ are found however in the range obtained from the Arrhenius plot of $(T_1)_{min}$ at the three frequencies (Figure 9). The discrepancy pointed out for $(\tau_R)_0$ is undoubtedly a consequence of the approximations involved in our theoretical calculations of T_1, namely the isotropic motion of the segments of the main chain, the uncertainties about the geometrical and conformational parameters, and the assumed invariance of Σr_{ij}^{-6} for the protons upon oscillation of the ring. Moreover in the study of the anisotropic motion of the pyridyl ring we have not considered the distribution correlation times τ_R and τ_G which would involve the adjustment of additional parameters. We have now however observed with some trial calculations that introducing a distribution of correlation times implies smaller oscillation angles. It seems therefore that our simplified treatment, while accounting for the dynamical behavior of the polymer under study, led to an overestimate of α which should not exceed 40° for $E_G \simeq 3$ kcal mol^{-1} according to conformational energy calculations.

(4) Contribution of the Cross Relaxation to the Estimate of Proton Spin–Lattice Relaxation Times. In the case of a homonuclear multispin system, the recovery of the longitudinal magnetization $(M_z)_i$ following at 180° pulse is not a single exponential of the time if cross relaxation occurs and has to be obtained by integration of a system of differential equations represented by[35-38]

$$\frac{d(M_z)_i}{dt} = \sum_j (\rho_{ij} + \sigma_{ij})[M_0 - (M_z)_i] + \sum_j \sigma_{ij}[(M_z)_i - (M_z)_j] \quad (8)$$

where M_0 is the equilibrium value of $(M_z)_i$ and $(M_z)_j$. We shall consider only the most simple case of an isotropic motion where the constants ρ_{ij} and σ_{ij} are given by equations[37,38]

$$\rho_{ij} = \frac{\gamma_H^4 \hbar^2 r_{ij}^{-6}}{10}\left(\tau_R + \frac{3\tau_R}{1+\omega_H^2\tau_R^2} + \frac{6\tau_R}{1+4\omega_H^2\tau_R^2}\right) \quad (9)$$

$$\sigma_{ij} = \frac{\gamma_H^4 \hbar^2 r_{ij}^{-6}}{10}\left(-\tau_R + \frac{6\tau_R}{1+4\omega_H^2\tau_R^2}\right) \quad (10)$$

at time $t = 0$, $(M_z)_i = (M_z)_j = -M_0$ so that

$$\left[\frac{d(M_z)_i}{dt}\right]_{t=0} = \tfrac{3}{5}\gamma_H^4\hbar^2 M_0 \sum_j r_{ij}^{-6}\left(\frac{\tau_R}{1+\omega_H^2\tau_R^2} + \frac{4\tau_R}{1+4\omega_H^2\tau_R^2}\right) = 2M_0T_1^{-1} \quad (11)$$

The value of the spin–lattice relaxation time T_1 defined by eq 2 is then given by the initial rate of recovery of the longitudinal magnetization. It should be obtained by the slope of the tangent at the origin of the semilogarithmic plot of $(S_\infty - S_i(t))/2S_\infty$ vs. time, $S_i(t)$ being the intensity of the signal of proton i at a time t after the 180° pulse and S_∞ being its asymptotic value. Except in the absence of cross relaxation where this plot is linear, this initial slope is somewhat difficult to determine experimentally. It may be approximated by the slope of log $(S_\infty - S_i(t))/2S_\infty$ in a time interval corresponding to a seemingly linear initial part of the plot. We have attempted to estimate to what extent this treatment is valid by taking into account the cross relaxation represented by the second term of eq 8. That has been done by integrating numerically three independent systems of nine differential eq 8 corresponding respectively to protons α and β of the chain and to proton 3 of the ring, each one being surrounded by the eight nearest neighbor protons mutually coupled by dipolar interactions. For the reasons given in section IV3 the protons 2 of the ring were not considered, except for their contribution to the cross relaxation of other protons. The parameters ρ_{ij} and σ_{ij} were calculated from interproton distances in the mr triad of the rrmrr sequence, in its minimum energy conformation provided by the SIMPLEX program. The integration of the differential system was performed by the Runge–Kutta's method[39] taking several values of τ_R between 10^{-10} and 10^{-8} s with $\omega_{H_1} = 6.28 \times 10^8$ rad s^{-1} (100 MHz) and $\omega_H = 1.57 \times 10^9$ rad s^{-1} (250 MHz). We have then compared the τ_R and T^{-1} dependence of the relaxation times T_1 of H_α, H_β, and H_3 given by eq 2 to the apparent T_1^* deduced from the computed recovery curves of the longitudinal magnetization taking the point where $(M_0 - (M_z)_i)/2M_0 = 0.5$. That seemed to us to correspond reasonably to our treatment of experimental semilogarithmic plots of $(S_\infty - S_{(t)})/2S_\infty$. As above, the temperature dependence of τ_R was defined by $E_R = 4$ kcal mol^{-1} and $(\tau_R)_0 = 1.3 \times 10^{-12}$ s.

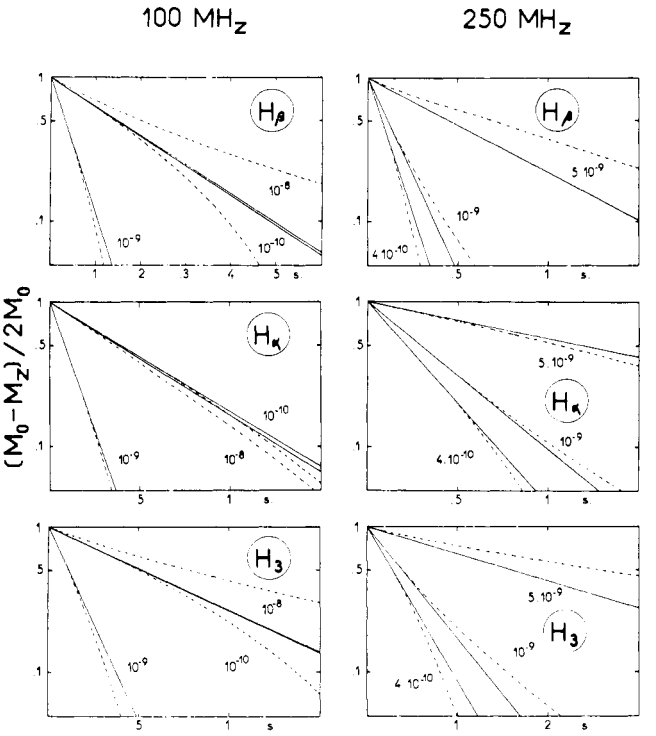

Figure 12. Some typical magnetization recovery curves computed for H_α, H_β, and H_3 at 100 and 250 MHz, with different values of τ_R, taking into account the cross relaxation (dotted lines). The tangents at the origin of these curves are given by solid lines.

In a recent paper Kalk and Berendsen[38] pointed out that for comparatively long correlation times and high Larmor frequencies, the cross-relaxation term of eq 8 becomes predominant and that the relaxation rates of all protons of a multispin system converge toward a common average value depending upon τ_R.

In the present case, our calculations show actually that the deviations of T_1^* from T_1 plots vs. T^{-1} (Figures 12 and 13) are as expected, more important at 250 MHz than at 100 MHz.

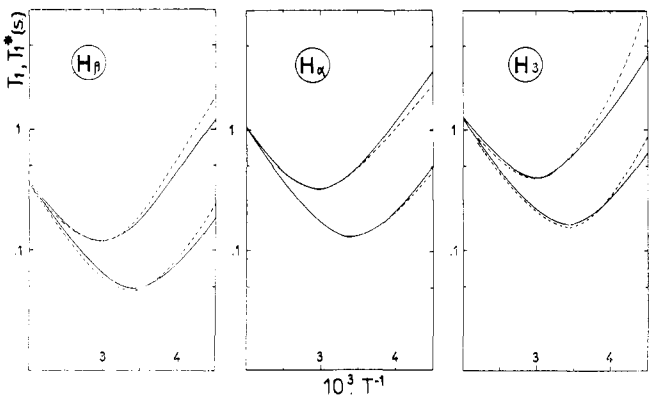

Figure 13. Comparison between the T^{-1} dependence of the spin–lattice relaxation time T_1 of H_α, H_β, and H_3 (solid lines) and of the apparent relaxation time T_1^* obtained by taking into account the cross relaxation (dotted lines). In each diagram the upper solid and dotted lines correspond to 250 MHz, the other lines to 100 MHz.

The apparent relaxation times of α and β protons are convergent but they do not coincide at 250 MHz even for $\tau_R = 10^{-8}$ s. This effect is however not experimentally observable since H_α and H_β resonances are superimposed. On the other hand, the apparent relaxation time of H_3 which is not as H_α, mainly relaxed by H_β, increases more rapidly with τ_R and T^{-1} than T_1, given by eq 2 for an isotropic motion. This behavior is inconsistent with the experimental observation and to the temperature dependence of T_1 calculated for our model of anisotropic motion of the pyridyl rings (Figure 11). Figure 13 shows moreover that even at 250 MHz the divergence of T_1^* and T_1 vs. T^{-1} curves computed for the three considered protons becomes significant only below 250 K and quite small at the vicinity of the minima. σ_{ij} passes indeed through zero for $\tau_R \simeq 1.12\omega_H^{-1}$ while $(T_1)_{min}$ corresponds to $\tau_R \simeq 0.62\omega_H^{-1}$. The rise of the minimum of the relaxation time of H_3 above the value predicted for an isotropic motion is therefore certainly not related to cross-relaxation effects since observed to a comparable extent at 100 and 250 MHz and even for ^{13}C (Figure 11). Likewise, the assumption of a distribution of correlation times to explain the temperature dependence of the relaxation time of H_α and H_β, which could be alternatively assigned to the influence of the cross relaxation, is well supported by the ^{13}C relaxation where this effect is removed by proton noise decoupling (see for instance ref 40).

In conclusion we may assume that the consideration of the cross relaxation between the protons of our polymer does not change fundamentally our interpretation of its dynamical behavior. Nevertheless it could have some influence on the choice of numerical values of the parameters involved in the simulation of the temperature dependence of the spin–lattice relaxation.

Appendix

We have previously studied the relaxation induced by oscillation motions of a rigid molecule in the solid state.[13] We shall now consider the case of molecule reorienting isotropically as a whole, with an oscillation internal motion.

The time-dependent parts of the dipole–dipole hamiltonian are:

$$F^{(0)} = r^{-3}(1 - 3n^2)$$
$$F^{(\pm1)} = r^{-3}(l \pm im)n$$
$$F^{(\pm2)} = r^{-3}(l \pm im)^2 \qquad \text{(A1)}$$

where l, m, and n are direction cosines of the inter-nuclear vector $\mathbf{r}$ with respect to the laboratory coordinate system $S(x,y,z)$.

Let $S_1(x_1,y_1,z_1)$ be the coordinate system fixed in the molecule. The time-dependent eulerian angles ψ, θ, and φ that transform the laboratory coordinate system S to S_1 describe the isotropic rotation of the whole molecule in S.

Without loss generality, one can fix the oscillating inter-nuclear vector $\mathbf{r}$ in a coordinate system $S_0(x_0,y_0,z_0)$ by the direction cosines:

$$l_0 = 0,\ m_0 = \sin\gamma, \text{ and } n_0 = \cos\gamma$$

γ being the angle between $\mathbf{r}$ and $\mathbf{z}_0$.

This yields

$$F_0^{(0)} = r^{-3}(1 - 3n_0^2) = r^{-3}(1 - 3\cos^2\gamma)$$
$$F_0^{(\pm1)} = r^{-3}(l_0 \pm im_0)n_0 = \pm\tfrac{i}{2}r^{-3}\sin 2\gamma$$
$$F_0^{(\pm2)} = r^{-3}(l_0 \pm im_0)^2 = -r^{-3}\sin^2\gamma \qquad \text{(A2)}$$

$\mathbf{z}_0$ is defined parallel to $\mathbf{z}_1$ which is taken as the oscillation axis. Thus the eulerian angles transforming S_1 to S_0 are ψ_1, 0, 0. The time-dependent angle ψ_1 describes the oscillation of $\mathbf{r}$ in S_1.

Using the transformation matrix elements we get eq A3 and A4.

$$A_m^{(n)} = e^{in\psi}g_m^{(n)}(\theta)e^{im\varphi} \qquad \text{(A3)}$$

with $g_m^{(n)}(\theta) =$

	m				
n	−2	−1	0	1	2
0	$-\frac{3}{4}\sin^2\theta$	$\frac{3}{2}\sin 2\theta$	$\frac{1}{2}(3\cos^2\theta - 1)$	$\frac{3}{2}\sin 2\theta$	$-\frac{3}{4}\sin^2\theta$
1	$-\frac{1}{4}\sin\theta(\cos\theta - 1)$	$\frac{1}{2}(2\cos^2\theta - \cos\theta - 1)$	$-\frac{1}{4}\sin 2\theta$	$\frac{1}{2}(2\cos^2\theta + \cos\theta - 1)$	$-\frac{1}{4}\sin\theta(\cos\theta + 1)$
2	$\frac{1}{4}(\cos\theta - 1)^2$	$\sin\theta(\cos\theta - 1)$	$-\frac{1}{2}\sin^2\theta$	$\sin\theta(\cos\theta + 1)$	$\frac{1}{4}(\cos\theta + 1)^2$

(A4)

One can write

$$F^{(q)}(t) = \sum_{p,r=-2}^{+2} A_p^{(q)}A_r^{(p)}F_0^{(r)}$$
$$= \sum_{p,r=-2}^{+2} A_p^{(q)}e^{ip\psi_1}g_r^{(p)}(0)F_0^{(r)}$$

with $g_r^{(p)}(0) = \delta_{pr}$, kronecker symbol

$$= \sum_{p=-2}^{+2} e^{iq\psi}g_p^{(q)}(\theta)e^{ip\varphi}e^{ip\psi_1}F_0^{(p)}$$

then the auto-correlation functions are:

$$G^{(q)}(t) = \langle F^{(q)*}(t)F^{(q)}(0)\rangle$$
$$= \sum_{p,p'=-2}^{+2} \langle e^{-iq\psi(t)}g_p^{(q)}(\theta(t))e^{-ip\varphi(t)}e^{-ip\psi_1(t)}F_0^{(p)*}$$
$$\times e^{iq\psi(0)}g_{p'}^{(q)}(\theta(0))e^{ip'\varphi(0)}e^{ip'\psi^1(0)}F_0^{(p')}\rangle \qquad \text{(A5)}$$

Assuming the independence of the two motions, one can separate the averaging in (A5):

$$G^{(q)}(t) = \sum_{p,p'=2}^{+2} \langle e^{-iq\psi(t)+iq\psi(0)} g_p{}^{(q)}(\theta(t)) \times g_{p'}{}^{(q)}(\theta(0)) e^{-ip\varphi(t)+ip'\varphi(0)} \rangle \times \langle e^{-ip\psi_1(t)+ip'\psi_1(0)} \rangle F_0{}^{(p)*} F_0{}^{(p')} \quad \text{(A6)}$$

The first average corresponds to isotropic rotational brownian motion and gives the well-known expression:

$$\langle g_p{}^{(q)}(\theta)^2 \rangle e^{-t/\tau_R} \delta_{pp'} \quad \text{(A7)}$$

where $\delta_{pp'}$ is the kronecker symbol and τ_R the correlation time of this motion.

The second average corresponds to the oscillational motion considered here.

In a similar way as Look and Lowe,[34] one can find the probability $P(i,f,t)$ that the internuclear $\mathbf{r}$ is in the position $\psi_1(t) = \psi_f$ at time t, given that it was in position $\psi_1(0) = \psi_i$ at time $t = 0$.

$$P(i,f,t) = \tfrac{1}{2}(1 + \epsilon e^{-t/\tau_G})$$

where τ_G is the correlation time of the oscillation motion and ϵ equals to +1 or −1 according to $\psi_1(t) = \psi_1(0)$ or $\psi_1(t) \neq \psi_1(0)$.

There are four possible situations to be taken into account for the second averaged factor: $\psi_1(t) = \psi_1(0) = \psi_i$; $\psi_1(t) = \psi_1(0) = \psi_f$; $\psi_1(t) = \psi_f$, $\psi_1(0) = \psi_i$; $\psi_1(t) = \psi_i$, $\psi_1(0) = \psi_f$.

At time $t = 0$, one assumes that the probabilities to find $\mathbf{r}$ in the positions defined by ψ_i and ψ_f are equal to:

$$p(0,\psi_i) = p(0,\psi_f) = \tfrac{1}{2}$$
$$(p(0,\psi_i) + p(0,\psi_f) = 1)$$

It follows:

$$\langle e^{-ip\psi_1(t)+ip'\psi_1(0)} \rangle = \left\langle \sum_{i,f} e^{-ip\psi_1(t)+ip'\psi_1(0)} P(i,f,t) p(0) \right\rangle$$

after averaging over all possible values of ψ_i and defining $\psi_f - \psi_i = \alpha$ as the oscillation amplitude one gets

$$\langle e^{-ip\psi_1(t)+ip'\psi_1(0)} \rangle = \tfrac{1}{2}\delta_{pp'}\{(1 + \cos p\alpha) + (1 - \cos p\alpha)\, e^{-t/\tau_G}\} \quad \text{(A8)}$$

Inserting (A7) and (A8) into (A6) one obtains the autocorrelation functions:

$$G^{(q)}(t) = \tfrac{1}{2} \sum_{p=-2}^{2} \langle g_p{}^{(q)}(\theta)^2 \rangle \{(1 + \cos p\alpha) e^{-t/\tau_R} + (1 - \cos p\alpha) e^{-t/\tau_t}\} |F_0{}^{(p)}|^2$$

where $\tau_t{}^{-1} = \tau_G{}^{-1} + \tau_R{}^{-1}$ and $\langle g_p{}^{(q)}(\theta)^2 \rangle$ is to be averaged over all space.

The spectral density is the Fourier transform of the autocorrelation function:

$$J^{(q)}(\omega_q) = \int_{-\infty}^{\infty} G^{(q)}(t) e^{-i\omega_q t}\, dt$$

After performing all calculations one obtains: (1) For homonuclear (½) spins I

$$T_1{}^{-1} = \tfrac{9}{8}\gamma_I{}^4\hbar^2 \sum_j r_{ij}{}^{-6}\{J^{(1)}(\omega) + J^{(2)}(2\omega)\}$$
$$= \tfrac{9}{80}\gamma_I{}^4\hbar^2 \sum_j r_{ij}{}^{-6}\{A(\alpha,\gamma_{ij}) f(\tau_R) + B(\alpha,\gamma_{ij}) f(\tau_t)\} \quad \text{(A9)}$$

with

$$A(\alpha,\gamma) = \tfrac{2}{3}(1 - 3\cos^2\gamma)^2 + \sin^2 2\gamma(1 + \cos\alpha) + \sin^4\gamma(1 + \cos 2\alpha)$$
$$B(\alpha,\gamma) = \sin^2 2\gamma(1 - \cos\alpha) + \sin^4\gamma(1 - \cos 2\alpha)$$
$$f(\tau) = \frac{\tau}{1 + \omega^2\tau^2} + \frac{4\tau}{1 + 4\omega^2\tau^2}$$

$$T_2{}^{-1} = \tfrac{9}{32}\gamma_I{}^4\hbar^2 \sum_j r_{ij}{}^{-6}\{J^{(0)}(0) + 10J^{(1)}(\omega) + J^{(2)}(2\omega)\}$$
$$= \tfrac{9}{160}\gamma_I{}^4\hbar^2 \sum_j r_{ij}{}^{-6}\{A(\alpha,\gamma_{ij}) g(\tau_R) + B(\alpha,\gamma_{ij}) g(\tau_t)\} \quad \text{(A10)}$$

with

$$g(\tau) = 3\tau + \frac{5\tau}{1 + \omega^2\tau^2} + \frac{2\tau}{1 + 4\omega^2\tau^2}$$

(2) For heteronuclear (½) spins I and S we have likewise

$$T_1{}^{-1}(\mathrm{I}) = \tfrac{1}{16}\gamma_I{}^2\gamma_S{}^2\hbar^2 r^{-6}\{J^{(0)}(\omega_I - \omega_S) + 18J^{(1)}(\omega_I) + 9J^{(2)}(\omega_I + \omega_S)\}$$
$$= \tfrac{3}{80}\gamma_I{}^2\gamma_S{}^2\hbar^2 r^{-6}\{A(\alpha,\gamma) h(\tau_R) + B(\alpha,\gamma) h(\tau_t)\} \quad \text{(A11)}$$

with

$$h(\tau) = \frac{\tau}{1 + (\omega_I - \omega_S)^2\tau^2} + \frac{3\tau}{1 + \omega_I{}^2\tau^2} + \frac{6\tau}{1 + (\omega_I + \omega_S)^2\tau^2}$$

$$T_2{}^{-1}(\mathrm{I}) = \tfrac{1}{32}\gamma_I{}^2\gamma_S{}^2\hbar^2 r^{-6}\{4J^{(0)}(0) + J^{(0)}(\omega_I - \omega_S) + 18J^{(1)}(\omega_I) + 36J^{(1)}(\omega_S) + 9J^{(2)}(\omega_I + \omega_S)\}$$
$$= \tfrac{3}{160}\gamma_I{}^2\gamma_S{}^2\hbar^2 r^{-6}\{A(\alpha,\gamma) k(\tau_R) + B(\alpha,\gamma) k(\tau_t)\} \quad \text{(A12)}$$

with

$$k(\tau) = 4\tau + \frac{\tau}{1 + (\omega_I - \omega_S)^2\tau^2} + \frac{3\tau}{1 + \omega_I{}^2\tau^2} + \frac{6\tau}{1 + \omega_S{}^2\tau^2} + \frac{6\tau}{1 + (\omega_I + \omega_S)^2\tau^2}$$

The nuclear overhauser enhancement is:

$$\mathrm{NOE} = 1 - \frac{\gamma_S}{\gamma_I} \frac{J^{(0)}(\omega_I - \omega_S) - 9J^{(2)}(\omega_I + \omega_S)}{J^{(0)}(\omega_I - \omega_S) + 18J^{(1)}(\omega_I) + 9J^{(2)}(\omega_I + \omega_S)}$$
$$= 1 - \frac{\gamma_S}{\gamma_I} \frac{A(\alpha,\gamma) l(\tau_R) + B(\alpha,\gamma) l(\tau_t)}{A(\alpha,\gamma) h(\tau_R) + B(\alpha,\gamma) h(\tau_t)} \quad \text{(A13)}$$

with

$$l(\tau) = \frac{\tau}{1 + (\omega_I - \omega_S)^2\tau^2} - \frac{6\tau}{1 + (\omega_I + \omega_S)^2\tau^2}$$

It may be pointed out that when the oscillational motion is much slower than the isotropic rotational motion, i.e., $\tau_G \gg \tau_R$, or when the oscillation amplitude α is equal to zero, one obtains easily from (A9) to (A13) the well-known corresponding expressions for the case of isotropic rotational motion.

On the other hand, if the isotropic rotational motion is much slower than the oscillational motion, i.e., $\tau_R \gg \tau_G$, one obtains the expressions for the case of a pure oscillational motion.

References and Notes

(1) (a) Service de Chimie Physique; (b) Laboratoire de Photophysique Moléculaire, CNRS, Orsay, France.
(2) (a) A. Allerhand and R. K. Hailstone, *J. Chem. Phys.*, **56**, 3718 (1972); (b) D. Doddrell, V. Glushko, and A. Allerhand, *ibid.*, **56**, 3683 (1972).
(3) A. Allerhand and E. Oldfield, *Biochemistry*, **12**, 3428 (1973).
(4) J. Schaefer and D. F. S. Natusch, *Macromolecules*, **5**, 416 (1972).
(5) J. Schaefer, E. O. Stejskal, and R. Buchdahl, *Macromolecules*, **8**, 291 (1975).
(6) Y. Inoue, A. Nishioka, and R. Chûjô, *Makromol. Chem.*, **168**, 163 (1973); *J. Polym. Sci., Polym. Phys. Ed.*, **11**, 2237 (1973).

(7) Y. Inoue and T. Konno, *Polym. J.*, **8**, 457 (1976).
(8) F. Heatley, *Polymer*, **16**, 493 (1975).
(9) F. Heatley and A. Begum, *Polymer*, **17**, 399 (1976).
(10) F. Laupretre and L. Monnerie, *Eur. Polym. J.*, **11**, 845 (1975).
(11) C. Chachaty, A. Forchioni, and J. C. Ronfard Haret, *Makromol. Chem.*, **173**, 213 (1973).
(12) D. Ghesquiere, C. Chachaty, Buu Ban, and C. Loucheux, *Makromol. Chem.*, **177**, 1601, 2567 (1976).
(13) Buu Ban and C. Chachaty, *Can. J. Chem.*, **51**, 3889 (1973).
(14) J. B. Berkowitz, M. Yamin, and R. M. Fuoss, *J. Polym. Sci.*, **28**, 69 (1958).
(15) G. Freeman and H. D. W. Hill, *J. Chem. Phys.*, **54**, 3367 (1970).
(16) M. Brigodiot, H. Cheradame, M. Fontanille, and J. P. Vairon, *Polymer*, **17**, 254 (1976).
(17) K. Matsuzaki, T. Kanai, T. Matsubara, and S. Matsumoto, *J. Polym. Sci., Part A*, **14**, 1475 (1976)
(18) G. M. Lukovkin, O. P. Komarova, V. P. Torchilin, and Yu. E. Kirsh, *Vysokomol. Soedin., Ser. A*, **15**, 443 (1973).
(19) W. Spendley, G. R. Hext, and F. R. Hinsworth, *Technometrics*, **4**, 441 (1962).
(20) J. A. Nelder and R. Mead, *Comput. J.*, **7**, 308 (1965).
(21) E. Ralston and J. L. Decoen, *J. Mol. Biol.*, **83**, 393 (1974).
(22) Kindly supplied by Dr. J. Thiery, Service de Biophysique, Cen, Saclay.
(23) C. Rerat, *Acta Crystallogr.*, **15**, 427 (1962).
(24) F. Jordan, *J. Am. Chem. Soc.*, **97**, 3330 (1975).
(25) V. P. Panov, V. V. Gusev, V. P. Dubrovin, and V. P. Yevdakov, *Vysokomol. Soedin., Ser. A*, **17**, 1782 (1975).
(26) Yu. E. Kirsh, O. P. Komarova, and G. M. Lukovkin, *Eur. Polym. J.*, **9**, 1405 (1973).
(27) P. Štrop, F. Mikeš, and J. Kálal, *J. Phys. Chem.*, **80**, 694 (1976).
(28) J. E. Anderson, K. J. Liu, and R. Ullman, *Discuss. Faraday Soc.*, **49**, 257 (1970).
(29) Yu. Ya. Gotlib, M. I. Lifshits, and V. A. Shevelev, *Vysokomol. Soedin., Ser. A*, **17**, 1360 (1975).
(30) J. J. Lindberg, I. Siren, E. Rahkamma, and P. Törmälä *Angew. Makromol. Chem.*, **50**, 187 (1976).
(31) R. A. Bonham, L. S. Bartell, and D. A. Kohl, *J. Am. Chem. Soc.*, **81**, 4765 (1959).
(32) T. M. Connor, *Trans. Faraday Soc.*, **60**, 1574 (1964).
(33) R. Lenk Rapport C. E. A., R-3651, 1969.
(34) D. C. Look and I. J. Lowe, *J. Chem. Phys.*, **44**, 2995 (1966).
(35) I. Solomon, *Phys. Rev.*, **99**, 559 (1955).
(36) J. S. Noggle and R. E. Schirmer, "The Nuclear Overhauser Effect. Chemical Applications", Academic Press, New York, N.Y. 1971.
(37) K. Akasaka, T. Imoto, S. Shibata, and H. Hatano, *J. Magn. Reson.*, **18**, 328 (1975).
(38) A. Kalk and H. J. C. Berendsen, *J. Magn. Reson.*, **24**, 343 (1976).
(39) H. Mineur, "Techniques de Calcul Numérique", Dunod, Paris, 1966.
(40) T. D. Alger, R. Freeman, and D. M. Grant, *J. Chem. Phys.*, **57**, 2168 (1972).

Carbon-13 NMR Observations of the Microstructure and Molecular Dynamics of Poly(phenylthiirane)

R. E. Cais* and F. A. Bovey

Bell Laboratories, Murray Hill, New Jersey 07974. *Received March 11, 1977*

ABSTRACT: We have examined the microstructure and molecular dynamics of three poly(phenylthiirane)'s in chloroform solution by ^{13}C NMR at 25.16 MHz. The aromatic quaternary and ortho carbon resonances were sensitive to triad stereosequences, whereas the backbone methine carbon resonance exhibited tetrad splittings. A sample prepared by "autopolymerization" was almost perfectly atactic (Bernoullian, with $P(m) = 0.48$), but heterogeneous catalysis with cadmium compounds produced fairly stereoregular polymers in which the stereosequence distributions conformed to first-order Markov statistics. Defect structures were also observed and assigned to head-to-head monomer placements. Measurements of ^{13}C spin–lattice relaxation times and nuclear Overhauser enhancements indicated that the polymer backbone was highly flexible, with motional correlation times about an order of magnitude shorter than those for polystyrene. Moreover, the results showed that the phenyl ring rotated with frequencies approximating 0.1 GHz, in strong contrast with the restricted motion of this group in polystyrene. Data obtained over the temperature range 10 to 55 °C gave apparent activation energies for segmental motions and phenyl rotation of 18 and 20 kJ/mol, respectively. The results are suggestive of cooperative local motions.

We have shown by ^{13}C NMR that in polymers of the class $[-CH_2CH(C_6H_5)-X-]$ both backbone carbons are sensitive to dyad tacticity and that the chain is substantially more flexible than that of polystyrene when X is a peroxide unit.[1] It was found that the phenyl group in the polyperoxide, unlike that of polystyrene, was able to rotate freely with a rate comparable to that for segmental reorientations along the backbone. In this paper, we extend our ^{13}C NMR studies to the system where X is sulfur, i.e., poly(phenylthiirane).

The structures of several polythiirane's have been examined by NMR. Most attention has been focussed on poly(methylthiirane), and studies by both proton[2,3] and ^{13}C[4,5] NMR have proved valuable in determining the effects of different polymerization catalysts on tacticity. Complete line assignments in the ^{13}C spectrum were made possible by the use of model compounds.[6] Irregular head-to-head structures in poly(methylthiirane) have been detected by ^{13}C NMR,[7-9] which has also been applied to structural studies of butyl, *tert*-butyl, phenyl,[4] and isopropyl[10] polythiirane's, and of 1,1-dimethylthiirane copolymers with thiirane and methylthiirane.[11] In particular, Ivin et al.[4] found for poly(phenylthiirane) that the quaternary and backbone methine carbons revealed dyad and triad stereosequences, respectively. Assignments of the configurational multiplets were made by a comparison of spectra of polymers obtained with different catalysts.

In contrast, there is very scanty NMR relaxation data for polythiiranes. Boileau et al.[7,8] measured ^{13}C T_1 values for poly(methylthiirane) at 25.16 MHz and 60 °C, as a method of confirming assignments in the ^{13}C spectrum. Their reported methine carbon T_1 value of 1.4 s indicates a highly flexible polymer with a motional correlation time approximating 35 ps. The present paper is concerned primarily with the correlation times for local motions in poly(phenylthiirane) in solution, as revealed by the spin–lattice relaxation times (T_1) and nuclear Overhauser enhancement factors (η). Some new structural assignments are also presented.

Experimental Section

Monomer. Phenylthiirane (styrene sulfide or 1,2-epithioethylbenzene) was prepared in 55% yield by the reaction of potassium thiocyanate with phenyloxirane (styrene oxide or 1,2-epoxyethylbenzene) in 50% aqueous dioxane solution, according to the procedure reported by Guss and Chamberlain.[12] The crude phenylthiirane was extracted with ether and isolated by removal of all volatiles boiling at 61 °C under 133 Pa of pressure; ^{13}C NMR showed that the product contained 13% of unreacted phenyloxirane. This mixture was distilled at 0.133 Pa to yield a middle fraction of 95% purity, containing 5%